Clay Minerals, (2014) **49**, 429–441

Coexistence of halloysite and iron-bearing clays in an altered ignimbrite, Patagonia, Argentina

F. CRAVERO[1,2,*], S. A. MARFIL[3,4], C. P. RAMOS[5] AND P. MAIZA[3]

[1] *Instituto de Geocronología y Geología Isotópica, CONICET-UBA, Pabellón INGEIS, Ciudad Universitaria, CABA, Argentina,* [2] *CONICET, Av. Rivadavia 1917, Buenos Aires, Argentina,* [3] *Department of Geology, Universidad Nacional del Sur, San Juan 670, Bahía Blanca, Argentina,* [4] *CIC of the Province of Buenos Aires, Street Nº 526 between 10 and 11, La Plata, Argentina, and* [5] *Departamento de Física de la Materia Condensada, GIyA–CAC–CNEA, Av. Gral. Paz 1499 (1650), San Martín, Buenos Aires, Argentina*

(*Received 19 September 2013; revised 11 April 2014; Editor: George Christidis*)

ABSTRACT: The Mamil Choique halloysite deposits of Patagonia, Argentina, contain randomly distributed green clay inclusions and patches within the halloysite mass. Halloysite has been formed from the thorough alteration of rhyolitic to dacitic ash fall tuffs and ignimbrites of the Huitrera Formation, Eocene age, under ambient conditions. The smectites present in the clay inclusions have been determined as ferruginous beidellites with variables amounts of Fe^{3+} in octahedral sites. The weathering activity that caused the formation of halloysite was also responsible for the genesis of the iron-bearing clay minerals, the formation of which was controlled mainly by permeability. Textural variations within the rock indicate favourable local geochemical environments for the formation of the green clay minerals.

KEYWORDS: iron-bearing smectites, halloysite, weathering, Patagonia, Argentina.

The Mamil Choique halloysite deposits of Patagonia, Argentina, contain green clay inclusions and patches which are randomly distributed in the halloysite mass. These inclusions and patches have rounded to irregular shape, their size varying from a few mm up to 1 m, and their contact with the halloysite mass is sharp. The green clay inclusions consist of a smectite-type clay mineral with a certain amount of iron content (Cravero *et al.*, 2009). As previously determined, halloysite is associated with minor kaolinite and cristobalite and has been derived from the thorough alteration of rhyolitic to dacitic ash fall tuffs and ignimbrites under ambient conditions (Cravero *et al.*, 2009, 2012).

* E-mail: fcravero@uns.edu.ar
DOI: 10.1180/claymin.2014.049.3.06

Halloysite forms under acid environments and in areas with high rainfall and good drainage, whereas smectite requires less adequately drained environments and more alkaline conditions. Kadir & Karakas (2002) attributed the formation of halloysite, kaolinite and Mg-smectites in different ignimbrite units to different geochemical environments produced by the variable permeability due to different textures.

Iron-rich smectites are known to form by weathering of basic rocks. Christidis (2008) pointed out the relationship between the composition of the bentonite parent rocks and the amount of Fe^{3+} per half unit cell (huc) in the derived smectite composition, thus indicating that smectites in bentonites derived from altered basic volcanic rocks are mainly Fe-montmorillonites and Fe-beidellites. Based on mineralogical and geological characteristics of different bentonite deposits, it has

© 2014 The Mineralogical Society

been suggested that Fe is present mainly as Fe^{2+} during smectite formation and hence may be mobilized during alteration (Christidis, 2008). Oxidation of Fe may take place when bentonites are exposed to more oxidizing conditions close to the surface.

Very few examples are known where nontronite or iron-rich smectites form from the alteration of acid rocks. The formation of nontronite in rhyolitic rocks has been described at early stages of alteration (Bernard *et al.*, 2004).

The aim of the present study was to determine the origin of the green clays randomly distributed as inclusions in the halloysite mass in the Mamil Choique deposits. In order to establish the geochemical environment needed for their formation, the type of smectite, its structural formula and chemical composition were determined.

MATERIALS AND METHODS

The Mamil Choique halloysite deposits are located in the southwest of Río Negro Province, ~80 km to the south of the town of Ingeniero Jacobacci (Fig. 1).

The clays studied are enclosed in the halloysite mass produced by weathering processes in the Eocene-Pliocene acting on volcanic-pyroclastic rocks of the Huitrera Formation of Eocene age (Cravero *et al.*, 2009, 2012). These rocks belong to the Eastern Belt of the Volcanic Andean Patagonian Province of Palaeocene–Eocene age, also known as the Andesitic Series (Pankhurst *et al.*, 2006). The green clay patches are randomly distributed and occur as irregular masses of different sizes ranging from a few mm up to 1 m.

Samples of the green clay inclusions, having different shapes and sizes, as well as the halloysitic clays that were in contact with them, were collected. The mineralogy, chemistry, morphology and origin of the hallosyite samples used here for comparison purposes have been already determined by Cravero *et al.* (2009, 2012).

The samples were labelled as: S1G: an irregular inclusion ~1 m in size enclosed in a S1W white halloysite matrix; S2G green: green lenticular clay, similar to S4G, enclosed in a white halloysite matrix (S2-4-5W); S3G: lenticular clay about 1 m long in contact with a white halloysite S3W; S4G: green lenticular clay about 10 cm in size in contact

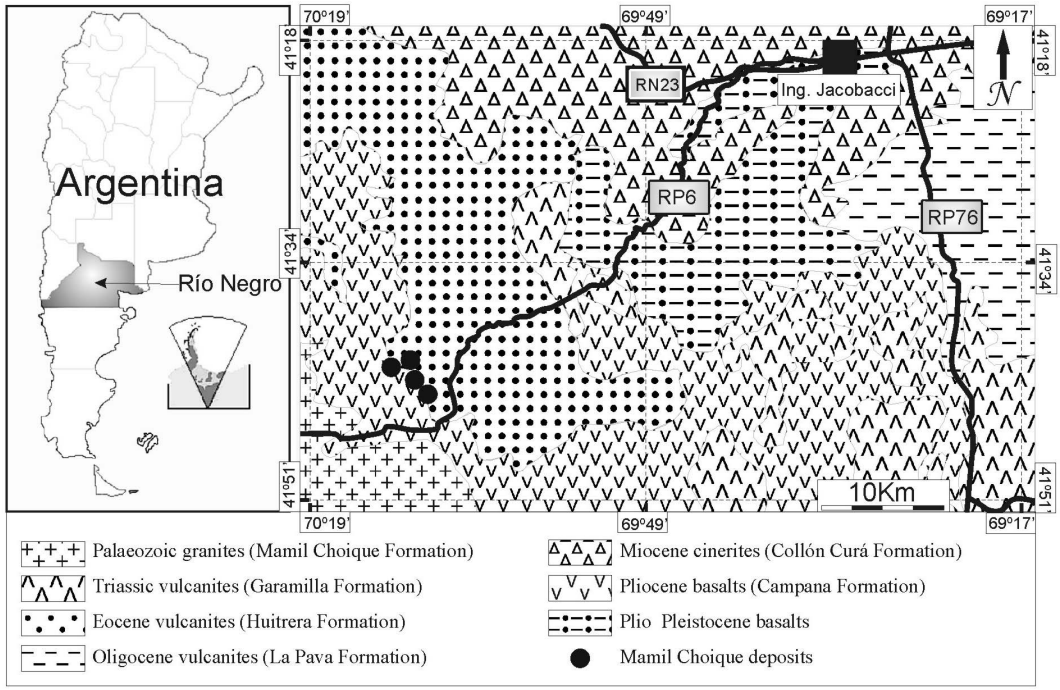

FIG. 1. Geological and geographical setting of the study area.

with a white halloysite (S2-4-5W); S5G: rounded inclusions less than 1 mm in size enclosed in a white halloysite mass (S2-4-5W) (Table 1).

Petrographic study as well as X-ray Diffraction (XRD), Differential Scanning Calorimetry (DSC), Fourier Transform Infrared (FTIR) spectroscopy, Mössbauer spectroscopy and chemical analyses were used to characterise the green clays. Petrographic determinations on thin sections were made with an Olympus B2-UMA trinocular petrographic microscope with a built-in Sony 151A video camera, a high-resolution monitor and Image-Pro Plus image. XRD analysis was performed using a Rigaku D-Max III diffractometer, with Cu-$K\alpha$ radiation and a graphite monochromator operating at 35 kV and 15 mA. XRD patterns were recorded on the whole rock from 3 to 70º2θ and on the <2 μm clay fraction from 3 to 15º2θ. DSC analysis was performed with a TA Q600 analyser under an inert atmosphere, at a heating rate of 10º/min from the ambient temperature up to 1000ºC. The FTIR spectra were obtained using a Nicolet 520 FTIR spectrometer. One mg of the samples was dispersed in 100 mg KBr and pressed in pellets. For each spectrum, 100 scans were recorded in the 400–4000 cm^{-1} spectral range with a resolution of 4 cm^{-1} in the transmittance mode.

Mössbauer spectra were obtained at room temperature (RT) with a conventional constant acceleration spectrometer in transmission geometry with a $^{57}Co/Rh$ source. Measurements were recorded at 7 mm/s and then fitted using the Normos program developed by Brand (1987). Isomer shift values are given relative to that of α-Fe at RT. Chemical analyses for major elements, performed by ACTLABS, Canada following their standarized procedures, were carried out on the green clay size samples by inductively coupled plasma mass spectrometry (ICP-MS).

RESULTS AND DISCUSSION

Petrography

The protolith is an ignimbrite with hyalopilitic texture, displaying welding foliation masked by argillization. Fractured crystal clasts, typical of pyroclastic rocks, include subhedral sanidine and corroded anhedral quartz (Fig. 2a). The alteration process is restricted to the glassy phase of the ignimbrite, with fresh sanidine crystal clasts. Depending on the permeability of the glass either halloysite or the green clays formed. Halloysite is found in areas of higher permeability where fluid flow is preserved and partially welded ash shards can be recognized. The green clay replaces irregular and/or lenticular massive vitroclasts of lower permeability (Fig. 2b).

The vitroclasts which were altered to the green clay are covered by cryptocrystalline silica and are surrounded by iron oxides. They are embedded in a halloysite groundmass. At the onset of alteration of these less permeable zones, migration of chemical elements was limited and a microenvironment, characterized by alkalis and iron concentration (higher pH), was formed (Fig. 2c). These conditions are favourable for the formation of the green clays and the excess silica and iron did not migrate but precipitated as cryptocrystalline quartz and iron oxides in the surroundings of the neoformed minerals. In places pseudomorphic selective replacement of pisoids by halloysite has been observed (Fig. 2d). The matrix is composed of green clays.

TABLE 1. Main characteristics of the studied samples.

Sample	Colour	Main characteristics
S1G	Green	Inclusion in halloysite mass ~1 m in size
S2G	Green	Lenticular mass
S3G	Green	Lenticular mass ~1 m long
S4G	Green	Lenticular mass ~10 cm in size
S5G	Green	Rounded inclusions <1 mm in size
S1W	White	Halloysite in contact with S1G
S2-4-5W	White	Halloysite in contact with S2G, S4G and S5G
S3W	White	Halloysite in contact with S3G

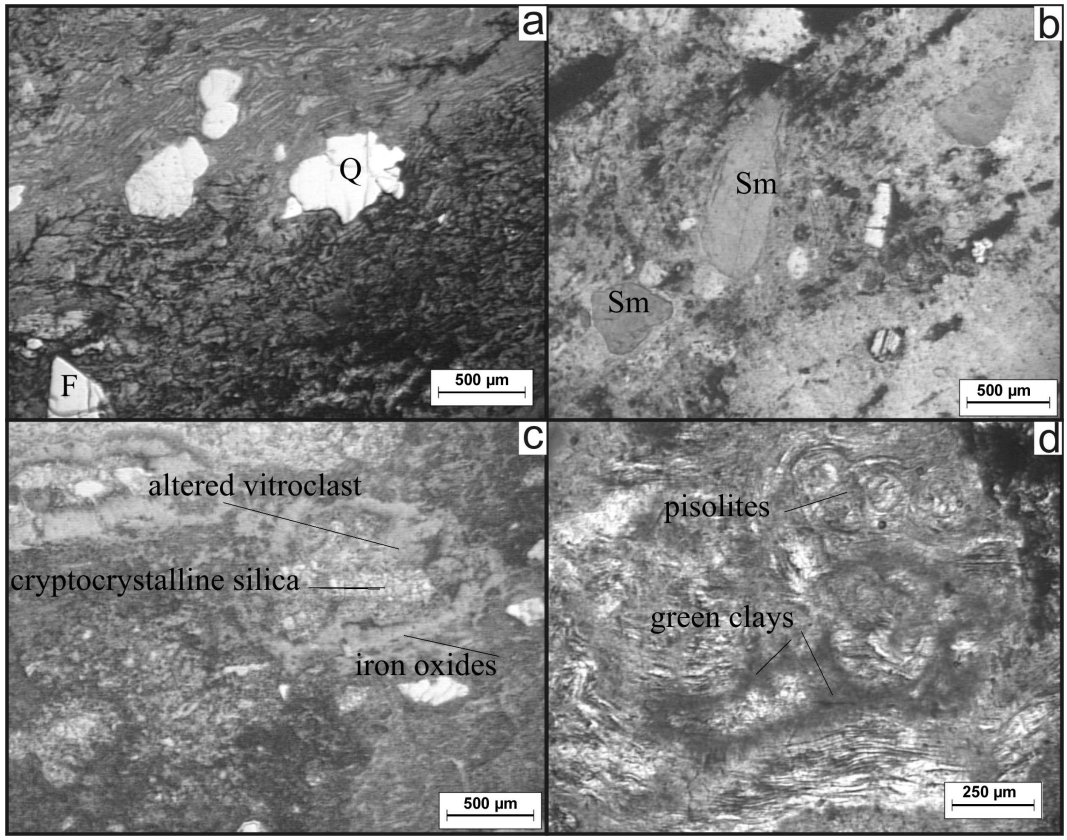

FIG. 2. Petrography of the fresh and altered source rock. Q = quartz, F = feldspar, Sm = smectites.

Clay mineral characterization

X-ray diffraction (XRD) data. The green clay samples are very pure, with traces of kaolinite and quartz in sample S3G and halloysite, quartz and feldspar in S4G. In all samples the smectite expands after ethylene glycol solvation from ~14 Å to 17 Å (Fig. 3b). Application of the Green-Kelly test did not yield unequivocal results. The 060 diffraction maximum at 1.50−1.51 Å indicates a dioctahedral-type clay mineral. In S3G the 060 maximum occurs at ~1.52 Å, indicating either a trioctahedral type or a nontronite (Fig. 4). Halloysite was positively identified by Cravero *et al*. (2009) after formamide intercalation.

Chemical analysis. The analysed clay size samples are characterized by a negative trend between Al_2O_3 and Fe_2O_3 indicating the possibility of substitution between them, the remaining major elements occurring at virtually constant concentrations (Table 2, Fig. 5).

The structural formula of the analysed clays varies from $(Si_{7.22}Al_{0.78})(Al_{2.88}Mg_{0.36}Fe_{0.78})(K_{0.06}Na_{0.42}Ca_{0.30})O_{20}(OH)_4$ with a tetrahedral charge of −0.78 e/uc and an octahedral charge of −0.34 e/uc for those with the lowest iron content (S1G and S5G), to $(Si_{7.20}Al_{0.80})(Al_{1.21}Mg_{0.26}Fe_{2.58})(K_{0.03}Na_{0.01}Ca_{0.18})O_{20}(OH)_4$ with a tetrahedral charge of ~−0.84 e/uc and an octahedral charge of −0.10 e/uc for those of the highest iron content (S3G) (Table 3). This indicates that 70% to 90% of the layer charge is tetrahedral. All the green clays studied have <3 mol.% of iron, some even less than 1 mol%.

Two types of Al-rich dioctahedral smectites exist depending on the localization of the layer charge: (a) montmorillonite where the charge arises mainly from substitution of Al by divalent cations, usually Mg, in the octahedral sites and (b) beidellites where the charge arises from the aluminium substitution for silicon in the tetrahedral sites. In ferruginous smectites Al is partially replaced by Fe^{3+}.

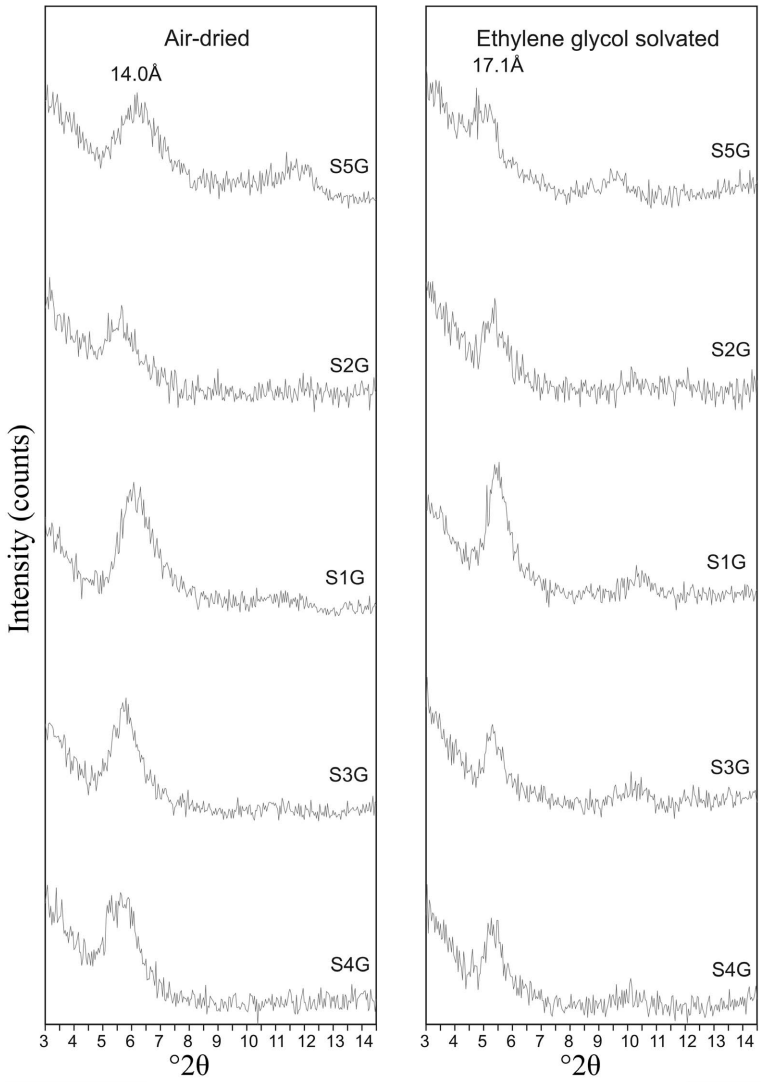

FIG. 3. XRD of green clay samples. Air dried and after ethylene glycol solvation.

Nontronites are the ferric members of dioctahedral smectites, most of which are structural counterparts of beidellites (Brindley, 1980). Köster *et al.* (1999) used the experimental limits defined in Güven (1988) to distinguish nontronite (>1.0 octahedral Fe per huc) and Fe-rich smectite (0.3−1.0 octahedral Fe per huc). In the ideal nontronite, the octahedral sheet consists entirely of Fe^{3+} ions, with the layer charge arising from substitution of Al^{3+} for Si^{4+} in the tetrahedral sheet, thus imparting a beidellitic character to the mineral. As with the other dioctahedral smectites, however, the ideal formula rarely corresponds to reality and some degree of divalent cation substitution in the octahedral sheet, usually Mg^{2+} often ocurrs. For practical purposes, nontronite is distinguished by octahehdral Fe^{3+} occupancy >1.5 per $O_{10}(OH)_2$ (Wilson, 2013, and references therein).

The clay minerals studied are dioctahedral smectites with layer charge stemming from substitution of Al for Si in the tetrahedral sites. The substitution of Al by Fe^{3+} in the octahedral sites varies from Fe^{3+} 2.58 (1.29 per huc) to 0.78

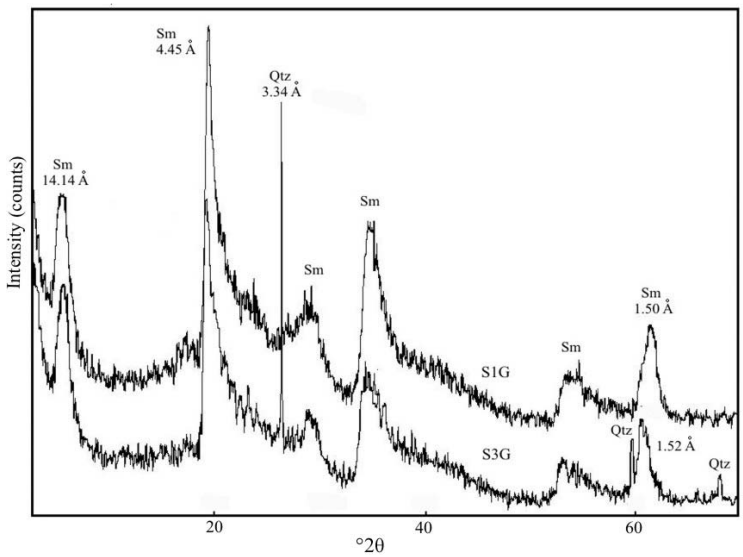

FIG. 4. XRD of selected samples. S1G with low iron content and S3G with the highest iron content. Qtz = quartz, Sm = smectite.

(0.30 per huc). These values correspond to Fe-rich smectites and are very close to the limits for nontronite and Fe-rich beidellite (Güven, 1988).

Bouna *et al*. (2012) considered a smectite with structural formula $(Si_{7.51}Al_{0.49})(Al_{2.99}Fe^{3+}_{0.68}Mg_{0.33})(Ca_{0.03}Na_{0.54}Mg_{0.11})O_{20}(OH)_4$ to be ferruginous beidellite.

The ferruginous smectite SWa-1 (CMS, Source Clay Minerals Repository) with structural formula $M^{+}_{0.95}(Al_{1.10}Fe_{2.61}Mg_{0.25})(Si_{7.40}Al_{0.60})O_{20}(OH)_4$ (Frost *et al*., 2000) is also beidellitic and is very similar to S3G with the highest iron content. The analysed clay minerals may be characterized as ferruginous beidellites. The main characteristic of the studied clays is that they have a relatively high Al content.

Differential scanning calorimetry (DSC) data. All samples showed a marked endothermic peak at 100ºC (Fig. 6) due to the loss of adsorbed water. A small weight loss at 200ºC observed in all the samples could be attributed to the overlap of the dehydration and dehydroxylation steps (Frost *et al*., 2000) or to the removal of strongly bound highly linked water.

A main endothermic peak in the temperature range 300−600ºC with a maximum around 480ºC (Fig. 6) is due to dehydroxylation with a corresponding weight loss of ~5%. Hohen-Hagen

TABLE 2. Major element composition of the studied samples (wt.%).

Sample	SiO_2	Al_2O_3	Fe_2O_3(T)	MnO	MgO	CaO	Na_2O	K_2O	TiO_2	P_2O_5	LOI	Total
S1G	45.67	19.58	6.59	0.009	1.49	1.38	0.28	0.09	0.204	0.17	24.59	100.00
S2G	43.67	17.05	11.76	0.006	1.01	1.73	0.21	0.07	0.091	0.13	24.8	100.50
S3G	43.04	10.26	20.46	0.008	1.02	2.02	0.19	0.12	0.067	0.04	22.67	99.89
S4G	44.51	23.96	8.10	0.002	0.92	1.40	0.10	0.04	0.052	0.04	21.29	100.41
S5G	48.58	23.97	6.57	0.009	0.64	0.94	0.52	0.42	0.430	0.05	18.11	100.25
S1W	43.57	29.41	1.36	0.009	0.24	0.30	0.12	0.24	0.927	0.06	23.44	99.68
S2-4-5W	42.61	28.36	1.21	0.007	0.12	0.19	0.08	0.08	1.67	0.04	23.88	98.24
S3W	47.45	29.12	3.78	0.013	0.45	0.46	0.22	0.18	0.198	0.07	17.27	99.22
Fresh rock	58.57	18.12	2.91	0.175	1.01	2.54	3.04	2.44	0.723	0.05	10.12	99.68

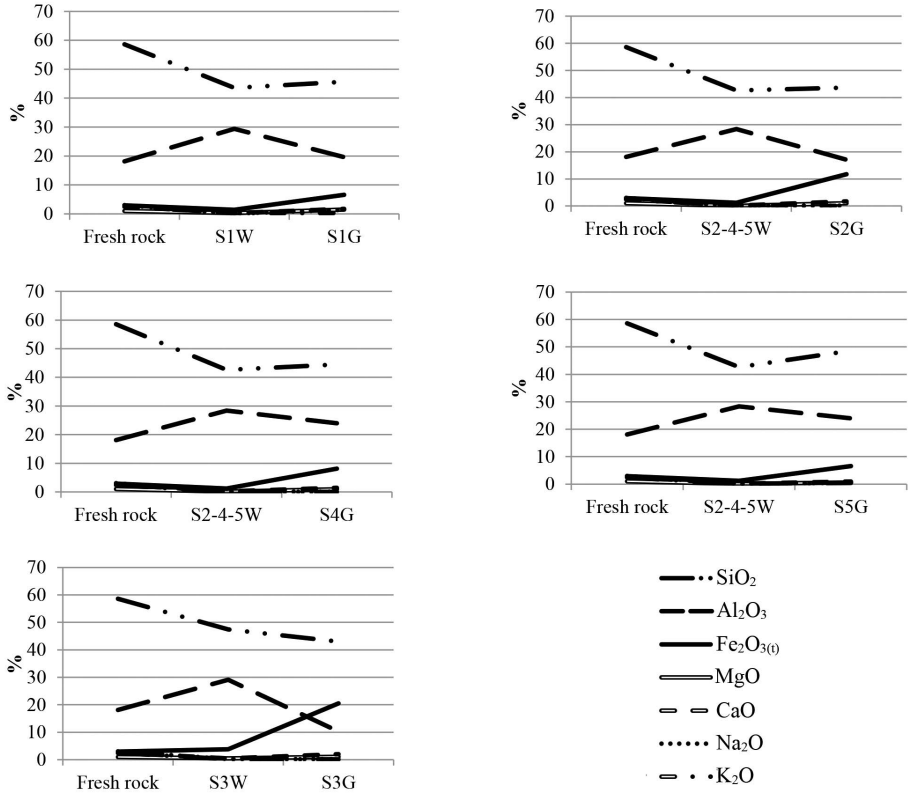

FIG. 5. Variations of the major chemical elements in the different green clays in relation with the fresh rock and the halloysite within which the green clay is enclosed

nontronite (NG-1 CMS standard), Uley nontronites (NAu-1 and NAu-2), Garfield nontronite (labelled as API-H33a, or sometimes H33a) and SWa-1 ferruginous smectite show a dehydroxylation endotherm centred at 450ºC (Frost *et al*., 2000). Che & Glotch (2012) reported a dehydroxylation temperature of 542ºC for SBCa-1 beidellite and 520ºC for NAu-1 nontronite, and Bouna *et al.* (2012) reported a dehydroxylation temperature of 510ºC for a ferruginous beidellite. Reported data for

TABLE 3. Sample description, structural formula and classification of the studied samples.

Sample	Description	Structural formula	Classification
S1G	Irregular mass ~1 m long	$(Si_{7.22}Al_{0.78})\ (Al_{2.88}Mg_{0.36}Fe_{0.78})_2$ $(K_{0.06}Na_{0.42}Ca_{0.30})O_{20}(OH)_4$	Ferruginous beidellite
S2G	Lenticular mass ~30 cm	$Si_{7.16}Al_{0.82})\ (Al_{2.46}Mg_{0.24}Fe_{1.16})_2$ $(K_{0.01}Na_{0.03}Ca_{0.15})O_{20}(OH)_4$	Ferruginous beidellite
S3G	Lenticular mass ~1 m long	$(Si_{7.20}Al_{0.80})(Al_{1.21}Mg_{0.26}Fe_{2.58})_2$ $(K_{0.03}Na_{0.01}Ca_{0.18})O_{20}(OH)_4$	Ferruginous beidellite
S4G	Lenticular mass ~10 cm long	$(Si_{6.82}Al_{1.19})(Al_{3.16}Mg_{0.22}Fe_{0.94})_2$ $(K_{0.008}Na_{0.02}Ca_{0.24})O_{20}(OH)_4$	Ferruginous beidellite
S5G	Rounded inclusions <1 mm	$(Si_{7.04}Al_{0.96})\ (Al_{2.72}Mg_{0.14}Fe_{0.74})_2$ $(K_{0.12}Na_{0.84}Ca_{0.60})O_{20}(OH)_4$	Ferruginous beidellite

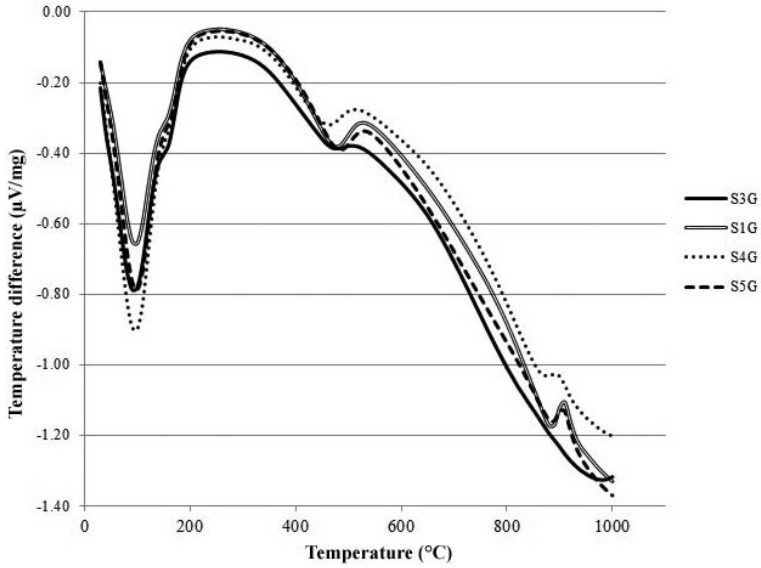

FIG. 6. DSC of the green clays.

beidellites indicate dehydroxylation temperatures of 560–600ºC (Weir & Green-Kelly, 1962; Post *et al*., 1997).

An exothermic peak at 920ºC, due to crystallization of a new anhydrous mineral phase, is present in all samples except the most ferruginous one S3G (Fig. 6). This temperature is close to that reported for an Fe-rich beidellite from the DeLamar-Florida Mountain mines (Post *et al*., 1997). This event is observed at higher temperatures in pure beidellites but is absent in nontronites or ferruginous smectites (Frost *et al*., 2000).

The dehydroxylation temperature at ~480º clearly indicates that the samples studied contain beidellite or nontronite in accordance with the mineral chemistry data. The 920ºC exothermic peak that is present in all the samples, except for S3G, suggests that the smectites are Fe-rich beidellites. S3G can also be considered as an Fe-rich beidellite.

Fourier transform infrared (FTIR) spectroscopy. The FTIR spectra of all samples except S2G are shown in Fig. 7a,b. S2G was excluded because its composition is almost identical to S5G (see XRD pattern). S3G exhibits an OH stretching vibration at 3565 cm^{-1}, which is present in SWa-1 ferruginous smectite (CMS, Source Clay Repository, Bishop *et al.*, 1999), and characteristic of nontronites with FeFeOH grouping dominating in the octahedral sheets (Madejová, 2003). The same band is also present in S1G but has much lower intensity. Sample S5G displays a band at 3696 cm^{-1} due to kaolinite/halloyiste contamination. The bands at 3620 cm^{-1} and at 915 cm^{-1}, present in the remaining samples, are characteristic of dioctahedral smectites and originate from AlAlOH stretching and bending vibrations respectively (Madejová, 2003; Bouna *et al.*, 2012). Sample S3G shows bands at 879 cm^{-1} and 816 cm^{-1}, assigned to AlFeOH and FeFeOH bending, respectively (Bishop *et al.*, 1999). The latter band is better defined in the sample with highest Fe content. The bands at 695 and 675 cm^{1} are attributed to Fe-O out-of-plane vibrations (Bishop *et al.*, 1999, Christidis, 2006). These data confirms that the study samples contain Fe-rich smectites.

Mössbauer spectroscopy. The Mössbauer spectra of sample SG1 with an Fe content less than 1 mol.% and SG3 which is richer in Fe were decomposed into two quadrupole doublets corresponding to Fe^{3+} cations in two different octahedral sites (Fig. 8a,b). These overlapping doublets, with similar isomer shift values (~0.37 mm/s) and quadrupole splittings in the range 0.3–0.4 mm/s for the inner doublet and ~0.7 mm/s for the outer doublet, are characteristic of iron-bearing smectites. The component with the smaller quadrupole splitting is conventionally associated with the site with *cis* OH groups (M2), since this site has the smaller electric field gradient based on point charge considerations, and the component with the larger

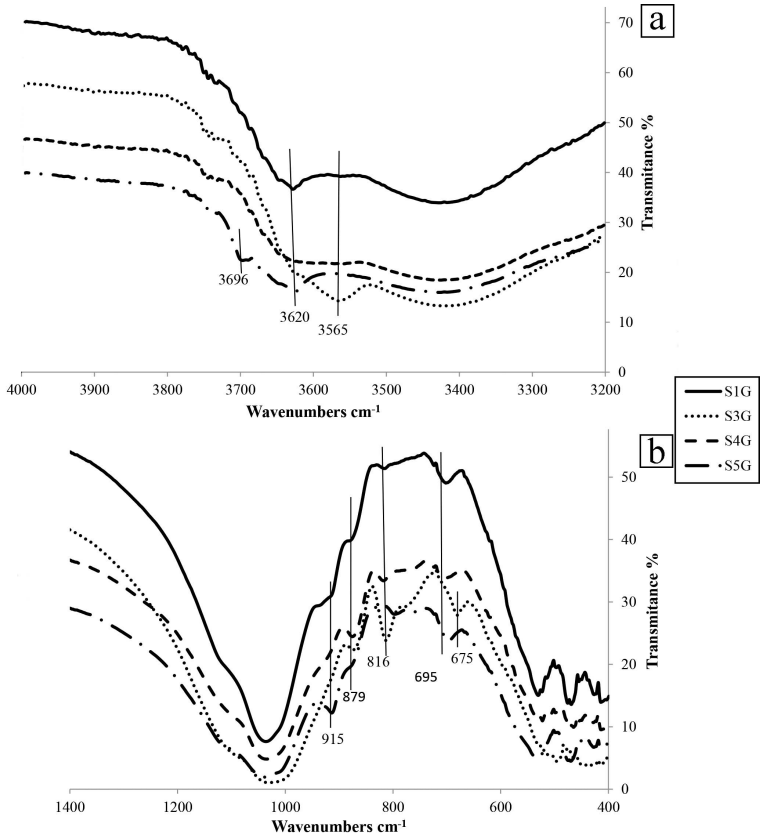

FIG. 7. FTIR of the studied samples. S2G was not included because its pattern is almost identical to S5G and was confusing.

quadrupole splitting is assigned to the site with *trans* OH groups (M1). The absolute ratio of the quadrupole splittings of Fe^{3+} in both configurations (M1 and M2) of dioctahedral smectites is approximately 1:2, as predicted by theory; this is demonstrated in the present case. Rozenson & Heller-Kallai (1977) showed that this ratio varies widely for the different types of smectites, showing that the octahedra are highly distorted in montmorillonites and beidellites, and considerably less distorted in nontronites. The magnitude of the quadrupole splitting of the M1 doublets is large for the montmorillonites and beidellitic smectites (QS values greater than 1 mm/s). Thus from Mössbauer spectra we can conclude that the iron-bearing smectites studied can be described as iron-rich beidellites tending to nontronites. From the comparison of the relative intensities of the Mössbauer lines, it is also possible to confirm that the S3G sample has the highest Fe^{3+} content (Fig. 8c), in agreement with a ferruginous smectite, closer to nontronite.

Origin

The green clays are enclosed in a halloysite matrix. This halloysite was formed from alteration of acid volcanic-pyroclastic rocks by weathering from Middle Eocene to Middle Oligocene (Cravero *et al.*, 2012). The alteration process in the white halloysite samples was characterized by the leaching of Si, alkalis and Fe, and residual enrichment of alumina (Cravero *et al*., 2009, 2012). The green clays are characterized by enrichment of iron and depletion of alkalis (Table 2, Fig. 5). Halloysite may form via weathering, pedogenesis or hydrothermal alteration of different types of rocks, i.e. ultramafic, mafic, rhyolitic rocks, volcanic glass and pumice (Joussein *et al*., 2005).

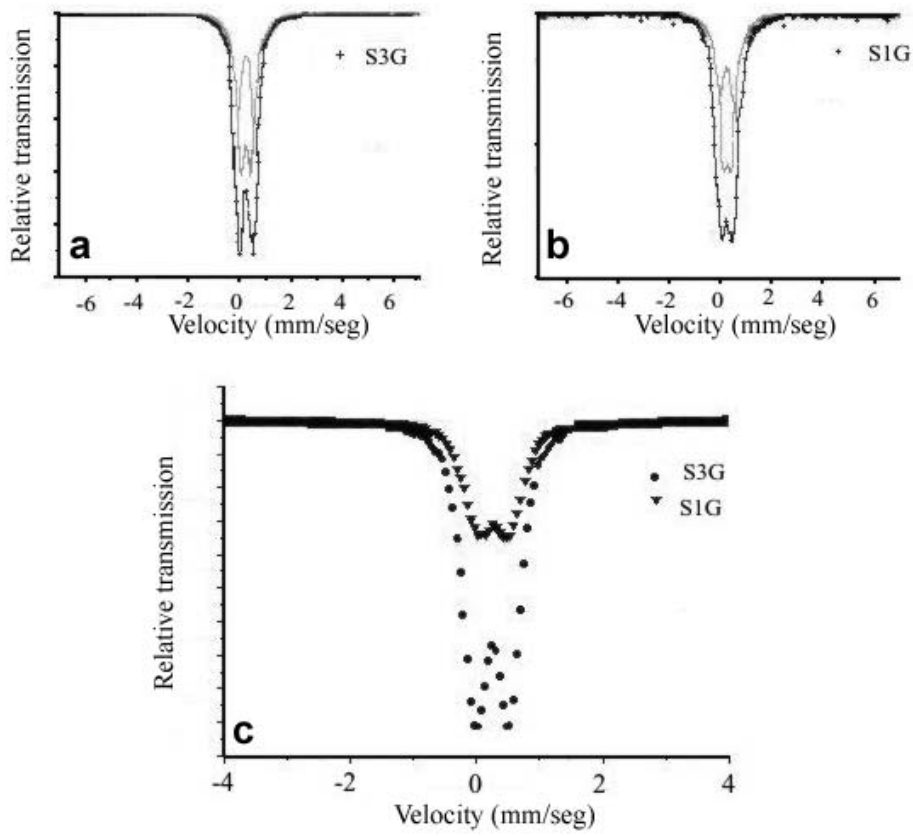

FIG. 8. Mössbauer spectra of sample (a) S3G, (b) S1G and (c) comparison between samples S1G and S3G.

A high water/rock ratio and an acidic environment, which favour the hydrolysis of silicates and volcanic glass, are favourable for halloysite. In the Mamil Choique area there is no evidence of vertical zonation that could indicate a downward alteration. It is probable that waters circulating towards small basins filled with these rocks came into contact with them for long periods of time, and halloysite instead of kaolinite formed after the dissolution of glass (Cravero *et al.*, 2012). There are no Fe or Mn oxides within the halloysite mass which would indicate a continuing flow of water during weathering (Churchman *et al.*, 2010).

Kaolinite is present in small amounts at Mamil Choique. It is generally considered that halloysite is transformed into kaolinite over time (Parham, 1969) and under favourable chemical conditions (Papoulis *et al*., 2004). Persistence of halloysite with time is related to climatic changes which led to arid conditions after halloysite formation (Cravero *et al.*, 2012). Fieldes & Williamson (1955) proposed a weathering sequence for rhyolitic tephra, which has been modified and widely accepted as follows: glass and feldspar to allophane and imogolite to halloysite and minor silica. Humid environments tend to produce allophane/imogolite, while halloysite is common in areas with distinct dry seasons and poor drainage (Mizota & van Reeuwijk, 1989).

Nontronite and iron-rich smectites usually form by alteration of basic rocks. Christidis (2006) studied bentonites where the smectite is an Fe-rich montmorillonite and Fe-rich beidellite with moderate Mg contents. Based on geological, mineralogical and chemical evidence he concluded that the smectites derived from intermediate to basic pyroclastic rocks, the high iron content of the smectite indicates a basic to intermediate origin. Iron-rich clay minerals have been found in subsoils under a wide range of climatic conditions such as rainfall variation of 300 to 3000 mm per year. A typical profile in a laterite

formed on basaltic rocks in Brazil shows a principal evolutionary trend for clay minerals (Oliveira *et al.*, 1998). Here there is a transition from smectite and mixed layer minerals that form green clays in the altered bedrock at the base of the profile to an intermediate association of nontronite and halloysite in the argillaceous alterite and finally to kaolinite in the mottled clay facies at the top of the profile.

The standard geochemical model of nontronite formation requires conditions that are initially sufficiently reducing for iron to remain in solution because Fe^{2+} is much more soluble than Fe^{3+}. This conclusion was also arrived at in synthesis studies; Harder (1978) found that only under *reducing conditions* could iron-bearing clay minerals be synthesized in a short time at low temperatures. The formation of the Fe^{3+}-bearing layer silicate minerals is only possible if Fe^{2+} is present in the solution during the formation of the silicate phase. It seems that high pH favours a rapid Fe clay mineral formation. Fe^{2+} or Mg in the solution stabilizes, as a mixed layer, the formation of the octahedral sheet built up mainly by Fe^{3+}. Christidis (2008) concluded that the variations in the properties of smectites can be explained if it is considered that Fe^{2+} is present when smectites are formed, and oxidized when the deposits are brought to the surface and make contact with pore waters.

The Fe-rich clays studied are characterized by a higher concentration of Fe_2O_3 when compared with both the source rock and the neoformed halloysite. Moreover the halloysite and the iron-rich clays have comparable SiO_2 contents and Al_2O_3 decreases in the iron-rich clays at the same rate as the Fe_2O_3 increases. Alkalis are enriched in the iron clays compared to halloysite (Table 2). Smectites derived from the alteration of basic rocks have, on average, 0.63 Fe^{3+} atoms per half unit cell (phuc), whereas those derived from intermediate and acidic rocks have, on average, 0.21 and 0.12 Fe^{3+} atoms phuc, respectively (Christidis, 2008). The Fe^{3+} content of the green clays varies from 0.39 to 1.79 which would suggest their origin from basic rocks. Nevertheless, the iron-rich clays are enclosed in a halloysite mass derived from a rhyolitic to dacitic ignimbrite that preclude a basic precursor, unless mafic inclusions were originally in the ignimbrite. Petrographic and field studies on the ignimbrite (Cravero *et al.*, 2012) have not shown any evidences of basic inclusions in these rocks; therefore, the iron-rich clays should have formed under special conditions from the acid precursor.

During weathering of basic rocks, iron-bearing minerals are very unstable and are readily altered, releasing iron in solution and forming Fe-rich smectites. In the case of weathering of acidic rocks, most of the minerals that are altered are not ferromagnesian; hence the main elements released into solution are alkalis. The fresh rock (ignimbrite) is poor in Fe (Table 2), suggesting that Fe has to be concentrated to form the Fe-rich clays. Smectites in bentonites derived from rocks whose composition varies from rhyolite to basaltic andesite vary considerably in composition on the micrometre scale (Christidis, 2006, 2008, and references therein). Compositional heterogeneity has been attributed to heterogeneity of the microenvironment during their formation (Christidis, 2006, and references therein). Composition in the microenvironment is an important parameter controlling the composition of the smectite, but the composition of the parent rock is also important (Christidis, 2008).

The presence of green clays in the halloysite groundmass can be explained if they formed from the same source rocks via a similar process as halloysite but under different pH-Eh conditions due to different permeability of the host rocks. During alteration of glass, Si, alkalis and Fe are released into solution. If the permeability is high, this fluid migrates leaving an Al-Si-rich residue that permits halloysite formation. If the permeability is low (such as in compact glass), the fluid cannot migrate and, as this reaction proceeds, pH increases. Eh has to be low in order to maintain Fe^{2+} in solution until it is locked in the structure of the iron-rich clays and later it is transformed to Fe^{3+}, when the clays come in contact with surface waters (Christidis, 2008). A low Eh may be attained in the water-saturated zone which is not in contact with air. The size of these zones containing green clays varies from microscopic areas (Fig. 9a) to 0.5 m in size (Fig. 9b). The Fe that is released into solution during halloysite formation and which does not participate in the smectite structure precipitates in the form of iron oxides in more permeable areas, which can be recognized as iron stains in the weathering profile.

Iron-rich clays show a variation in composition, depending on the availability of iron, which however was not adequate to form pure nontronite. Nontronite formation occurs at the early stages of the lateritization of a rhyolite in the Paraná Basin (Bernard *et al.*, 2004). In this case the complete weathering of the rock operated over a few

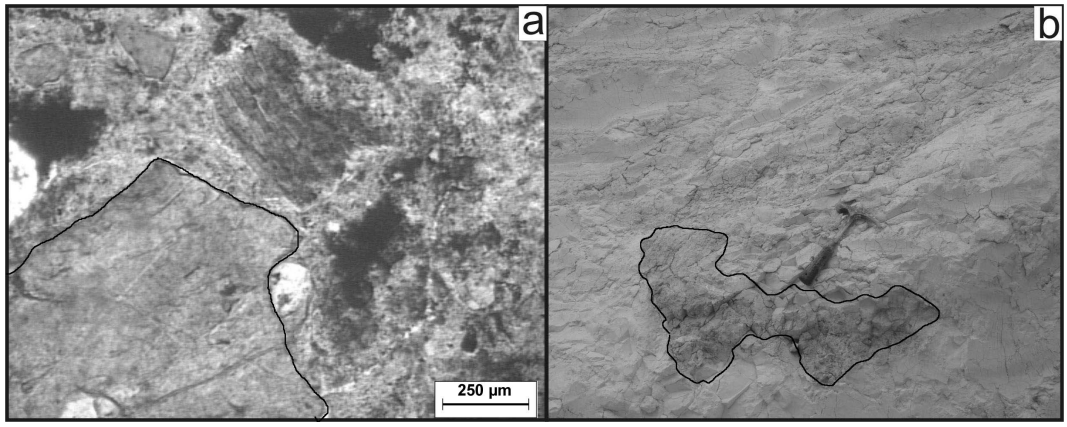

FIG. 9. Green clay patches. (a) Microscopic patch. (b) Irregular green patch in the halloysite mass.

centimetres only, following three successive steps: (a) K-nontronite crystallization in the fresh and massive rock, replacing glass and celadonite along the first meteoric fluid passways; (b) pervasive and complete dissolution of the plagioclases accompanied by a local and slight dissolution of glass in the grey alteration halo; and (c) massive crystallization of halloysite as the main constituent of the soil.

Kadir & Karakas (2002) observed that permeability controlled the formation of halloysite, kaolinite and smectites in Miocene ignimbrites of Konya, Turkey, but the different clay minerals are associated with different rock units and not with the same rock-type as in the present case. The present study demonstrated that halloysite and iron-bearing clays can be formed from weathering of an acid rock. The variable permeability within the rock, which also depends on the textural variations that produce different geochemical environments, is the main controlling factor of the alteration.

CONCLUSIONS

Two conclusions can be drawn from the present study.

1. The ferrouginous beidellites enclosed in a halloysite mass in the Mamil Choique deposits of Patagonia, Argentina, were formed by the alteration of acid volcanic-pyroclastic rocks from weathering during the Middle Eocene - Middle Oligocene.

2. Variations in the permeability of the host rock created microenvironments favourable for the formation of iron-rich clays, which is the main controlling factor in the alteration.

ACKNOWLEDGMENTS

The authors wish to thank the INGEIS - CONICET, CIC from the Province of Buenos Aires and the Geology Department of the Universidad Nacional del Sur for their helpful support during the research. We would like to thank the Principal Editor for his assistance and recommendations. The suggestions and recommendations of both anonymous reviewers improved the paper, especially the detailed revision of reviewer #1.

REFERENCES

Brindley G.W. (1980) Order-disorder in clay minerals. Pp. 125–195 in: *Crystal Structures of Clay Minerals and their X-ray Identification.* (G.W. Brindley & G. Brown, editors). Mineralogical Society of London, Monograph no. 5.

Bernard M., Dudoignon P. & Dani N. (2004) Dévitrification et altération supergène d'une rhyolite (Bassin du Paraná, Brésil): mécanismes et bilans géochimiques. *Comptes Rendus Geoscience*, **336**, 789–798.

Bishop J.L., Murad E., Madejová J., Komadel P., Wagner U. & Scheinost A.C. (1999) Visible, Mössbauer and infrared spectroscopy of dioctahedral smectites: Structural analyses of the Fe-bearing smectites Sampor, SWy-1 and SWa-1. *11th International Clay Conference*, June, 1997, Ottawa, 413–419.

Bouna L., Rhouta B., Daoudei L., Maury F., Amjoud M., Senocq F., Lafont M.C., Jada A. & Aghzzaf A.A. (2012) Mineralogical and physico-chemical characterizations of ferruginous beidellite-rich clays from Agadir Basin (Morocco). *Clays and Clay Minerals* **60**, 278–290.

Brand R.A. (1987) Normos program, Internat. Rep. Angewandte Physik, University of Duisburg.

Che C. & Glotch T.D. (2012) The effect of high temperatures on the mid-to-far-infrared emission and near-infrared reflectance spectra of phyllosilicates and natural zeolites: Implications for Martian exploration. *Icarus*, **218**, 585−601.

Christidis G.E. (2006) Genesis and compositional heterogeneity of smectites. Part III: Alteration of basic pyroclastic rocks. A case study from the Troodos Ophiolite Complex, Cyprus. *American Mineralogist*, **91**, 685−701.

Christidis G.E. (2008) Do bentonites have contradictory characteristics? An attempt to answer unanswered questions. *Clay Minerals*, **43**, 515−529.

Churchman G.J., Pontifex I.R. & McClure S.G. (2010) Factors influencing the formation and characteristics of halloysites or kaolinites in granitic and tuffaceous saprolites in Hong Kong. *Clays and Clay Minerals*, **58**, 220−237.

Cravero F., Martínez G.A. & Pestalardo F. (2009) Yacimientos de halloysita en Mamil Choique, Provincia de Río Negro, Patagonia. *Revista de la Asociación Geológica Argentina* **65**, 586−592.

Cravero F., Maiza P.J. & Marfil S.A. (2012) Halloysite in Argentinian deposits: origin and textural constraints. *Clay Minerals*, **47**, 329−340.

Fieldes M. & Williamson K.I. (1955) Clay Mineralogy of New Zealand Soils: Part I − Electron Micrography. *New Zealand Journal of Science and Technology*, **37**, 314−335.

Frost R.L., Ruana H., Kloprogge J.T. & Gates W.P. (2000) Dehydration and dehydroxylation of nontronites and ferruginous smectite. *Thermochimica Acta*, **346**, 63-72.

Güven N. (1988) Smectites. Pp. 497−559 in: *Hydrous Phyllosilicates (Exclusive of Micas)* (S.W. Bailey, editor). *Reviews in Mineralogy*, **19**. Mineralogical Society of America, Washington D.C.

Harder H. (1978) Synthesis of iron layer silicate minerals under natural conditions. *Clays and Clay Minerals*, **26**, 65−72.

Joussein E., Petit S., Churchman J., Theng B., Righi D. & Delvaux B. (2005) Halloysite clay minerals − a review. *Clay Minerals*, **40**, 383-426.

Kadir S. & Karakas Z. (2002) Mineralogy, chemistry and origin of halloysite, kaolinite and smectite from Miocene ignimbrites, Konya, Turkey. *Neues. Jahrbuch fur Mineralogie Abhandlungen*, **177**, 113−132.

Köster H.M., Ehrlicher U., Gilg H.A., Jordan R., Murad E. & Onnich K. (1999) Mineralogical and chemical characteristics of five nontronites and Fe-rich smectites. *Clay Minerals*, **34**, 579−600.

Madejová J. (2003) FTIR techniques in clay mineral studies. *Vibrational Spectroscopy*, **31**, 1−10.

Mizota C. & Van Reeuwijk L.P. (1989) *Clay mineralogy and chemistry of soils formed in volcanic material in diverse climatic regions*. Soil Monograph, **2**, ISRIC, Wageningen. 186 pp.

Pankhurst R.J., Rapela C.W., Fanning C.M. & Marquez M. (2006) Gondwanide Continental collision and the origin of Patagonia. *Earth-Science Reviews*, **76**, 235−257.

Papoulis D., Tsolis-Katagas P. & Katagas C. (2004) Progressive stages in the formation of kaolinite from halloysite in the weathering of plagioclase. *Clays and Clay Minerals*, **52**, 271−285.

Parham W.E. (1969) Halloysite-rich tropical weathering products of Hong Kong. *Proceedings of the International Clay Conference*, Tokyo, **1**, 403−416.

Post J.L., Cupp B.L. & Madsen F.T (1997) Beidellite and associated clays from the DeLamar Mine and Florida Mountain Area, Idaho. *Clays and Clay Minerals*, **45**, 240−250.

Rozenson I. & Heller-Kallai L. (1977) Mössbauer spectra of dioctahedral smectites. *Clays and Clay Minerals* **25**, 94−101.

Sherman G.D., Ikawa H., Uehara G. & Okazaki E. (1962) Types of occurrence of nontronite and nontronite-like minerals in soils. *Pacific Science*, **16**, 58−62.

Weir A.H. & Green-Kelly R. (1962) Beidellite. *American Mineralogist*, **47**, 137−146.

Wilson M.J. (2013) Nontronite. Pp 279−299 in: *Rock-forming Minerals: Sheet Silicates: Clay Minerals*, Volume 3C, 2nd edition. Geological Society of London.